Journal of Marine Systems 154 (2016) 192–205

Contents lists available at ScienceDirect

Journal of Marine Systems

journal homepage: www.elsevier.com/locate/jmarsys

Seasonality of vertical flux and sinking particle characteristics in an ice-free high arctic fjord—Different from subarctic fjords?

Ingrid Wiedmann [a,*], Marit Reigstad [a], Miriam Marquardt [a,b], Anna Vader [b], Tove M. Gabrielsen [b]

[a] UiT The Arctic University of Norway, Breivika, 9037 Tromsø, Norway
[b] The University Centre in Svalbard (UNIS), 9171 Longyearbyen, Norway

ARTICLE INFO

Article history:
Received 30 January 2015
Received in revised form 30 September 2015
Accepted 5 October 2015
Available online 23 October 2015

Keywords:
Gel trap
Particulate organic carbon (POC)
Particle size spectra
Aggregate
Detritus
Glacial runoff

ABSTRACT

The arctic Adventfjorden (78°N, 15°E, Svalbard) used to be seasonally ice-covered but has mostly been ice-free since 2007. We used this ice-free arctic fjord as a model area to investigate (1) how the vertical flux of biomass (chlorophyll *a* and particulate organic carbon, POC) follows the seasonality of suspended material, (2) how sinking particle characteristics change seasonally and affect the vertical flux, and (3) if the vertical flux in the ice-free arctic fjord with glacial runoff resembles the flux in subarctic ice-free fjords. During seven field investigations (December 2011–September 2012), suspended biomass was determined (5, 15, 25, and 60 m), and short-term sediment traps were deployed (20, 30, 40, and 60 m), partly modified with gel-filled jars to study the size and frequency distribution of sinking particles. During winter, resuspension from the seafloor resulted in large, detrital sinking particles. Intense sedimentation of fresh biomass occurred during the spring bloom. The highest POC flux was found during autumn (770–1530 mg POC m^{-2} d^{-1}), associated with sediment-loaded glacial runoff and high pteropod abundances. The vertical biomass flux in the ice-free arctic Adventfjorden thus resembled that in subarctic fjords during winter and spring, but a higher POC sedimentation was observed during autumn.

1. Introduction

Fjords have recently been identified to sequester a high amount of organic carbon (Smith et al., 2015), but global warming affects these high latitude marine ecosystems. Hitherto, seasonally ice-covered fjords may turn into year-round ice-free fjords, and it is largely unknown how ecological processes and glacial runoff may change and impact the downward flux of particulate organic carbon (POC) in these fjords.

The POC flux at high latitudes is generally characterized by a strong seasonality. Nutrient availability, phytoplankton concentration, and zooplankton biomass oscillate throughout the year (Leu et al., 2011; Rat'kova and Wassmann, 2002; Węsławski et al., 1991), resulting in a variable abundance of the most prominent vehicles of the vertical POC flux, i.e., algal aggregates, fecal pellets, and marine snow (Turner, 2002, 2015). Ice algae, which tend to form blooms in seasonally ice-covered seas and fjords during spring (Ji et al., 2013; Leu et al., 2011), are utilized by zooplankton (Søreide et al., 2010; Weydmann et al., 2013), but they also contribute to the vertical export, when the algal cells are released into the water column during melting and ice break-up (Arrigo, 2014; Tremblay et al., 1989). Phytoplankton spring blooms, dominated by diatoms, occur in April–May in ice-free waters or subsequent to ice break-up in seasonally ice-covered regions (Eilertsen and Frantzen, 2007; Leu et al., 2011) and may cause major biomass sedimentation events (Thompson et al., 2008; Wassmann et al., 1991). Senescent diatom cells and diatom resting stages have high sinking velocities (Rynearson et al., 2013; Smayda, 1971), and some taxa release sticky exopolymeric substances, which contribute to the formation of algal aggregates (Kiørboe et al., 1994; Thornton, 2002) and marine snow, i.e., conglomerates (>0.5 mm) of diverse composition and structure (Alldredge and Silver, 1988; Lampitt, 2001). These coagulation processes increase the particle size, which, in turn, can enhance the sinking velocity and the vertical POC export. However, the phytoplankton bloom in the Barents Sea as well as in fjords in northern Norway and around Svalbard may also be dominated by the prymnesiophyte *Phaeocystis pouchetii* (Degerlund and Eilertsen, 2010). This small flagellate has a single cell stage and a mucous colonial stage, but it tends not to promote aggregate formation (Passow and Wassmann, 1994), and its contribution to the vertical carbon flux below 60 m is low, despite sometimes high cell abundances in the water column (Reigstad and Wassmann, 2007; Reigstad et al., 2000).

Irrespective of the phytoplankton composition, strong vertical carbon flux can only occur when the top-down regulation is weak, i.e., when sinking biomass is not substantially grazed by zooplankton (Reigstad et al., 2000). In this scenario, large sinking particles may be

* Corresponding author at: UiT The Arctic University of Norway, 9037 Tromsø, Norway. Tel.: +47 776 44214.
E-mail address: Ingrid.Wiedmann@uit.no (I. Wiedmann).

http://dx.doi.org/10.1016/j.jmarsys.2015.10.003

less frequently fragmented into small, slowly sinking material by sloppy feeding (Noji et al., 1991; Svensen et al., 2012), which results in an higher biomass flux. Conversely, weak top-down regulation also reduces the re-packaging of small particles into fast-sinking zooplankton fecal pellets (Turner, 2002, 2015; Wexels Riser et al., 2008), contributing to a weak vertical biomass flux.

Apart from the biological processes, the surrounding environment, such as, e.g., terrestrial runoff, impacts the vertical carbon flux in fjords. Glacial runoff entrains lithogenic material with a high specific weight. When sinking particles "scavenge" this material, the sinking velocity of the organic material increases and results in an enhanced vertical biomass flux (Passow and De La Rocha, 2006).

It is largely unclear how these interacting seasonal processes of the plankton community and the environment will translate into vertical biomass flux in future arctic fjords. To address this question, we conducted a 9-month field study in the arctic Adventfjorden (78°N, 15°E, Fig. 1), western Svalbard. The fjord was previously seasonally ice-covered but has mostly been ice-free since 2007 (www.met.no) and may thus serve as a model area to study the mechanisms of vertical flux in an ice-free but glacially influenced arctic fjord. Our aim was to investigate the following: (1) how the vertical flux of organic matter follows the seasonal pattern of suspended material, (2) how sinking particle characteristics change with season and are linked to the vertical flux, and (3) if the vertical flux in an ice-free arctic fjord with major glacial runoff during autumn differs from the vertical flux in boreal and subarctic ice-free fjords.

2. Materials and methods

2.1. Study site and sampling program

The present study was conducted at station IsA (Isfjorden-Adventfjorden, 78°15.67′N, 15°32.10′E, Fig. 1) at the mouth of the arctic Adventfjorden. Adventfjorden is an approximately 8 km long, 3.5 km wide, and less than 100 m deep side branch of Isfjorden, a large fjord system on the western coast of Svalbard. Neither Isfjorden nor Adventfjorden has a sill at the fjord mouth, and they are therefore exposed to advection from the Atlantic-influenced West Spitsbergen Current. Warmer and more saline water from this current reached the study site (approximately 50 km from the open coast) and allowed year-round ship-based sampling in ice-free waters. Glacial runoff (Advent River, Longyear River, Fig. 1) affected IsA during the summer and autumn, bringing substantial amounts of sediment-loaded melt water (e.g., 9×10^6 m^{-3} during September, Węsławski et al., 1999).

Field investigations were conducted throughout 9 months, starting December 14, 2011, and ending September 19, 2012. We refer to the winter sampling days in December, mid-January, and late January as Winter I, Winter II, and Winter III (Table 1). Spring sampling days in late April, mid-May, and late May are denoted Spring I, Spring II, and Spring III, and the mid-September sampling is referred to as Autumn I (Table 1).

2.2. Hydrographic, light, and wind data

Hydrographical data included temperature and salinity measurements by a CTD (SD204, SAIV A/S, Bergen, Norway) and subsequent computation of the potential density. The seasonal light cycle at 78°N includes the polar night from mid-November to late January. The sun is below the horizon from early October to early March, and the midnight sun appears between mid-April and late August. Underwater irradiance was quantified using a handheld LI-1000 Data Logger (LI-COR, Nebraska, USA), and the euphotic zone was defined as the layer of >1% surface irradiance. Boat drift due to strong wind events made vertical deployment of the irradiance logger difficult, and an overestimation of the euphotic zone may be assumed. Wind data from Longyearbyen airport (78°14′N, 15°28′E, Fig. 1) are considered to be

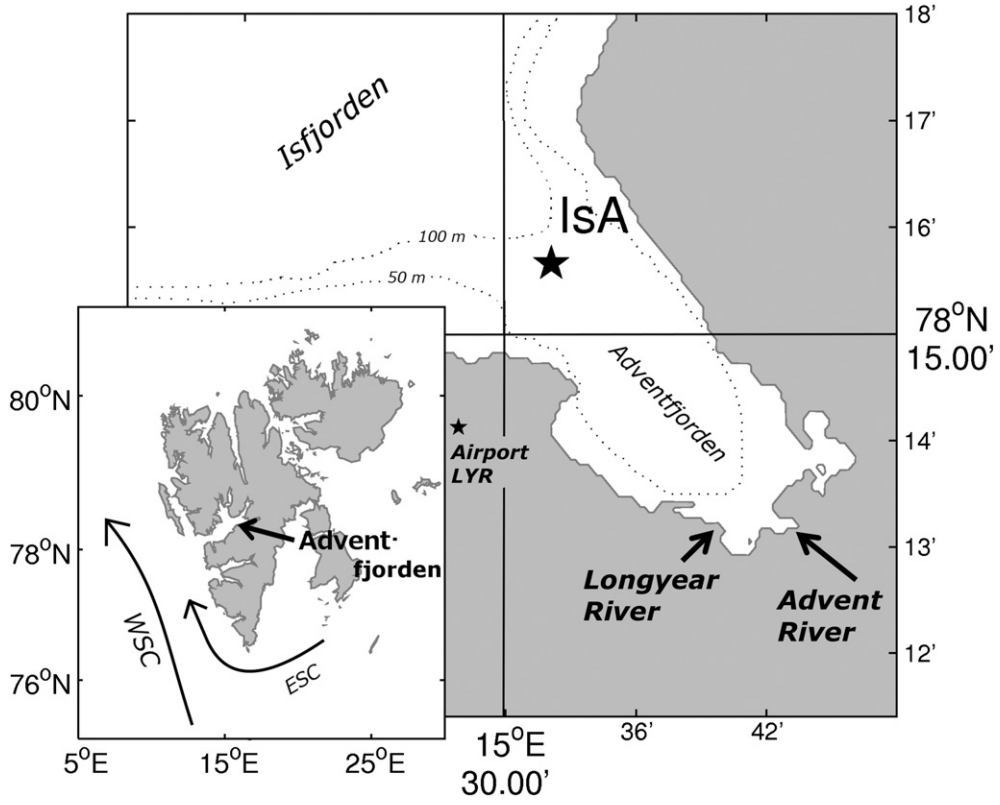

Fig. 1. IsA station was located in the mouth of Adventfjorden, a side branch of the Isfjorden system, western Svalbard (main map, depth contour according to Zajączkowski et al., 2010). Adventfjorden is influenced by the Atlantic-derived, warm West Spitsbergen Current (WSC) and the Arctic-derived, cold East Spitsbergen Current (ESC, small map), as well as glacial runoff from Longyear River and Advent River (during the ice melt period in summer and autumn).

Table 1
Sampling schedule for deployment of suspended water samplers, sediment traps, and "gel traps" (sediment traps modified with a gel jar) at IsA station (78°15.67′N, 15°32.10′E). Research Vessel: (1) *K/V Svalbard*, (2) *R/V Helmer Hanssen*, (3) *Polar Circle*, (4) *R/V Viking Explorer*, and (5) *M/V Farm*.

Label	Date	Boat	CTD	Euphotic zone (m)	Susp. Chl *a*, POC (mg m^{-3})	Susp. C/N	Deployment time (h)	Sediment trap[a] (m)	"Gel trap" (m)
Winter I	December 13/14, 2011	1	X		5,15,25,60	5,15,25,60[b]	24:15	20,30,40,60	20,30,40,60
Winter II	January 17/18, 2012	2	X		5,15,25,60	5,15,25,60	22:00	20,30,40,60	
Winter III	January 27/28, 2012	1	X		5,15,25,60	5,15,25,60	25:00	20,30,40,60	
	February 9, 2012	3	X		25				
	February 16, 2012	3	X		25				
	February 23, 2012	3	X		25				
	March 1, 2012	3	X		25				
	March 8, 2012	3			25				
	March 19–22, 2012[c]	3	X	34					
	March 29, 2012	3	X	45	25				
	April 3, 2012	3	X	40	25				
	April 11, 2012	3	X	40	25				
	April 16, 2012	3	X	45	25				
	April 23, 2012	3	X	35	25				
Spring I	April 26/27, 2012	4	X	30	5,15,25,60	5,15,25,60	24:25	20,30,40,60	
	April 30, 2012	3	X	30	25				
	May 3, 2012	3	X	25	25				
	May 7–9, 2012[c]	3	X	25	25				
Spring II	May 10/11, 2012	4	X	25	5,15,25,60	5,15,25,60	23:25	20,30,40,60	
	May 11, 2012	4					02:00		20,30,40,60
	May 16, 2012	3	X						
	May 24, 2012	3	X	30	25				
Spring III	May 30/31, 2012	4	X	20	5,15,25,60	5,15,25,60	23:45	20,30,40,60	
	May 31, 2012	4					01:50		20,30,40,60
	June 14, 2012	3	X		25				
	June 21, 2012	3		25	25				
	July 6, 2012	3	X	8	25				
	August 6, 2012	3	X	30	25				
	August 23, 2012	3	X	20	25				
	September 6, 2012	3	X						
Autumn I	September 18/19, 2012	5	X	30	5,15,25,60	5,15,25,60	23:05	20,30,40,60	
	September 19, 2012	5					02:30		20,30,40,60
	October 31, 2012	3	X		25				

[a] Analyzed for particulate organic carbon (POC), particulate organic nitrogen, and chlorophyll *a* (Chl *a*).
[b] Particulate organic nitrogen samples not available.
[c] Daily sampling.

representative for the IsA station and were downloaded from the Norwegian Meteorological Institute (www.eklima.met.no).

2.3. Suspended biomass (Chl a, POC, particulate organic nitrogen)

Seawater samples were collected at 5, 15, 25, and 60 m with a 10 L Niskin bottle, transferred into carboys, and stored dark and cool until filtration within a few hours (Table 1). Triplicates of 250–400 mL were vacuum-filtered on Whatman GF/F filters for analysis of the Chl *a* concentration. Filters were frozen in liquid nitrogen or at −80 °C until analysis within 9 months. Some pigment breakdown during the storage period may be assumed (Mantoura et al., 1997). Chl *a* was extracted 20–24 h in 10 mL methanol (in darkness, +4 °C), and concentrations were then measured in a Turner Design AU-10 fluorometer (calibrated with Chl *a*, Sigma S6144). For POC and particulate organic nitrogen analysis, triplicate subsamples (300–500 mL) were filtered on pre-combusted Whatman GF/F filters, stored at −20 °C, and analyzed within 2.5 years on a Leeman Lab CHN Analyzer according to the procedures described by Reigstad et al. (2008).

2.4. Vertical flux characterization (Chl a, POC, particle size spectra)

An anchored short-term sediment trap array was used to study the vertical flux of particulate material at IsA (Table 1). Paired trap cylinders (KC Denmark, d = 7.2 cm, 45 cm high, no baffles or poison) were mounted at 20, 30, 40, and 60 m and deployed for approximately 24 h (Table 1). In this way, we collected particles sinking out from the lower eutrophic zone and through the water below it (Table 1), and we minimized the sampling of re-suspended material from the seafloor (approximately 80 m). After the trap array was recovered, water from one of the paired cylinders from each depth was transferred into carboys. Subsamples were filtered to determine the vertical flux of Chl *a* and POC as described above for the suspended samples (duplicates or triplicates of 150–400 mL for Chl *a*, duplicates or triplicates of 250–500 mL for POC). The second trap cylinder at each depth was modified with a gel-containing glass jar that perfectly fits inside the trap cylinder (conceptual idea presented by Lundsgaard et al., 1999; with modification from polyacrylamide to commercially available unpoisonous gels as described by Thiele et al., 2015 and Wiedmann et al., 2014). Samples from these traps were used to study the vertical flux of particles ≥50 μm ESD_{image} (estimated spherical diameter determined from images) by an image analysis (concept presented by Ebersbach and Trull, 2008; Wiedmann et al., 2014). The threshold function of ImageJ (AutoThresholding following Otsu clustering algorithm, Otsu, 1979) was applied to establish a border between the particle and background in the 8-bit gray-converted images. Particles <50 μm ESD_{image} were excluded due to abundance underestimation of these particles (Jackson et al., 1997, 2005). The remaining particles were binned in 20 bins from 0.050 mm to 5.080 mm ESD_{image} (Table A1), and an ellipsoidal particle shape was assumed to estimate the particle volume (Wiedmann et al., 2014). The sediment trap deployment time was adjusted for the season (Table 1). During Winter I–III, we deployed the traps for approximately 24 h. During spring and autumn, the trap array was first deployed for approximately 24 h to determine the biogeochemical flux, and then for approximately 2 h to study the particle flux using gel-modified cylinders (short deployment prevented particle overload in the gels).

2.5. Calculation of the loss rate and sinking velocity

The loss rate can be expressed as the ratio of the vertical flux (POC, Chl *a* at depth z) to the integrated suspended biomass (POC, Chl *a*

above depth z). For the calculation of loss rates, the integrated suspended biomass was estimated by trapezoidal integration. Similarly, the average sinking velocity was expressed as the ratio of the vertical flux (mg m^{-2} d^{-1}) to the suspended biomass (mg m^{-3}) at depth z (Kiørboe et al., 1994).

3. Results

3.1. Hydrography, light regime, and wind

The hydrographic environment at station IsA (Fig. 2) reflected the seasonal pattern of the region. Cooling of the entire water column took place until mid-January, when warmer, denser, and more saline water from the West Spitsbergen Current was advected to IsA. Another cooling period took place in April and resulted in low water temperatures that persisted throughout May (−0.5 °C to 1.0 °C). Warming of the surface layers started in June, and maximum surface water temperatures were reached in late August, coinciding with enhanced glacial melt water runoff and a freshening of the surface water layers (August 23, 2012: maximum water temperature 6.4 °C, minimum salinity 31.5). Low air temperatures cooled the surface waters from September onward, while deeper water layers in the fjord remained warm into late October (<4.1 °C, Fig. 2). As glacial runoff tapered off during autumn, surface salinity increased (Fig. 2). Light was measured from March 8, 2012, onwards, when the sun rose above the horizon. Irradiance measurements indicated a euphotic zone ranging down to 20–40 m (Table 1), with the exception of a very shallow euphotic zone of 8 m on July 6, 2012. Wind data from Longyearbyen airport (Fig. 1) showed a prevailing wind direction "out of Adventfjorden" (6 of 7 sampling periods had a wind direction of E to SSW, data not shown). The opposite wind direction ("into Adventfjorden") was only observed during Spring III.

3.2. Suspended biomass (Chl a, POC) and its C/N ratio

The high-frequency sampling of the suspended biomass parameters Chl *a* and POC showed clear seasonal patterns (Fig. 2d). The Chl *a* and POC concentrations were low during winter, increased and peaked during the spring period (late April to end of May), and showed a decreasing trend throughout summer and autumn. These data provided a seasonal framework for our seven sampling events and indicated that Winter I–III, Spring I–III, and Autumn I (Fig. 2, blue lines) were typical representatives for seasonal scenarios with low, high, and intermediate suspended Chl *a* and POC concentrations. In addition, the vertical distribution of the suspended biomass concentration during the sampling events (Fig. 3) indicated a mixed water column during Winter I–III and Autumn I, but a vertical pattern during Spring I–III. A seasonal trend was observed in the quality of the particulate organic material reflected through (atomic) C/N ratios. Fresh material of algal origin is expected to reflect the Redfield ratio (C/N = 6.6), but a C/N ratio close to Redfield was only observed during Spring I–III. During Winter II and III and Autumn I, C/N ratios of 8.3–12.1 indicated that the biomass in the water column consisted of partly degraded material or a mixture of fresh marine material and biomass of terrestrial origin (terrestrial material C/ N > 17, Bianchi, 2006).

3.3. Vertical biomass flux (Chl a, POC) and its C/N ratio

The vertical flux patterns of Chl *a* and POC reflected a seasonality, partly matching the observations for the suspended material. During Winter I–III, vertical Chl *a* and POC flux were relatively low

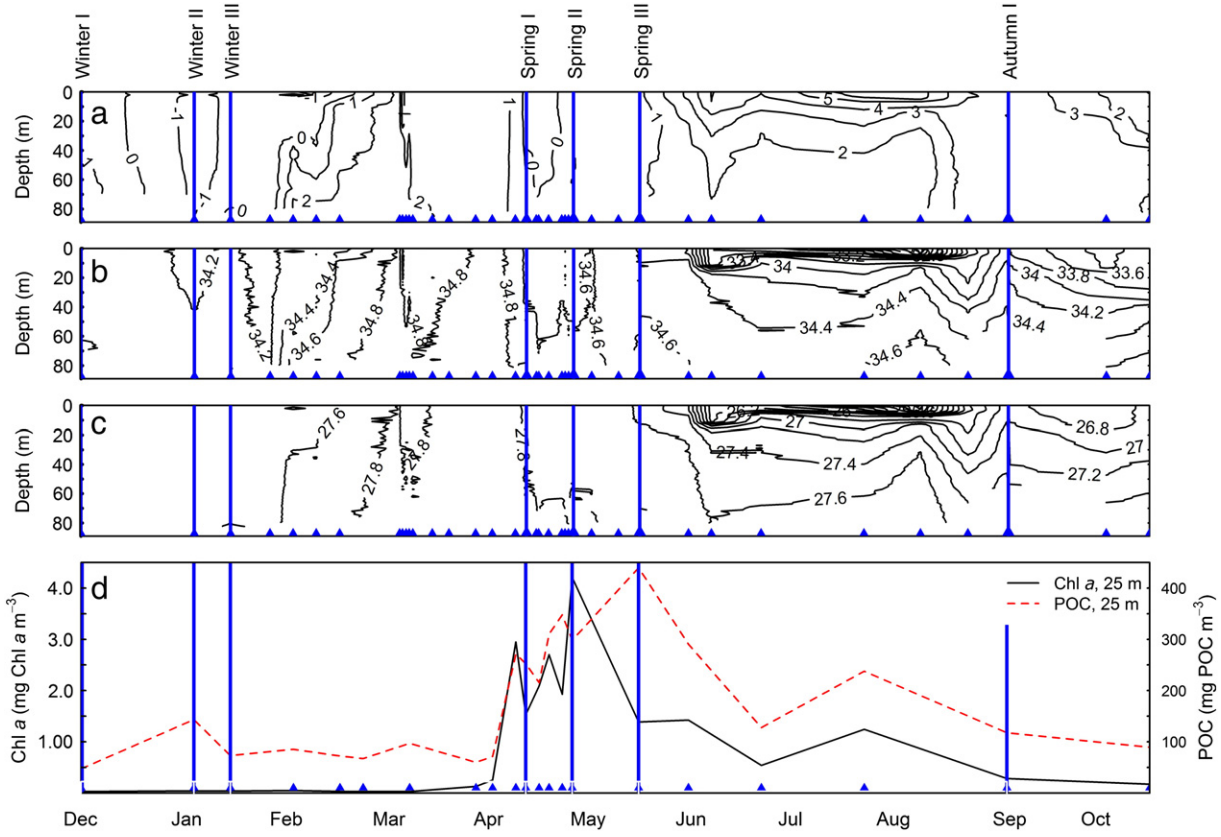

Fig. 2. Temperature (a), salinity (b), density (c), and the seasonal development of suspended biomass (d, black line: chlorophyll *a*, Chl *a*, red stippled line: particulate organic carbon, POC) at IsA during the sampling program (December 14, 2011 to October 31, 2012). Dates of CTD sampling are indicated by blue triangles. Sediment trap deployment took place on the dates indicated by vertical blue lines.

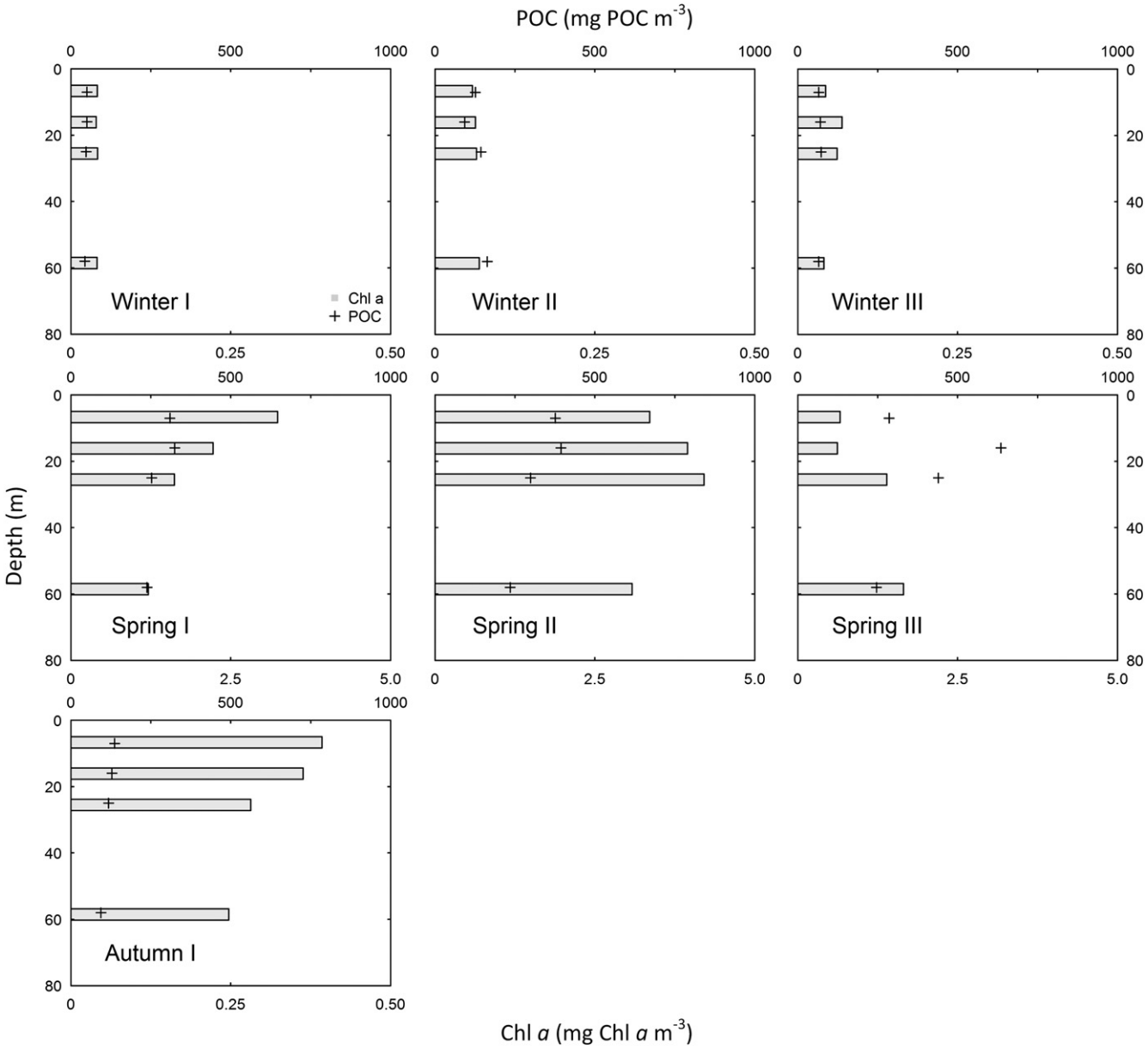

Fig. 3. Concentrations of suspended chlorophyll *a* (Chl *a*) (gray bars) and particulate organic carbon (POC, black crosses) at 5, 15, 25, and 60 m during Winter I–III, Spring I–III, and Autumn I. Note different scales on the lower *x*-axis for Spring I–III.

(90–140 mg POC m^{-2} d^{-1} and <0.26 mg Chl *a* m^{-2} d^{-1}, Fig. 4) but indicated that biomass flux also occurred during the polar night. The highest POC fluxes were measured during Winter II in the deepest traps, implying a resuspension event rather than sinking POC produced in the water column. The highest vertical Chl *a* fluxes were found during Spring I–II, when vertical POC fluxes also were high (>1000 mg POC m^{-2} d^{-1}), but the maximum vertical POC flux (1530 mg POC m^{-2} d^{-1}) was found during Autumn I (Fig. 4). Generally, the loss rates of Chl *a* and POC were higher at 30 m than at 60 m (exception Winter III, Table 2), while the sinking velocities were always higher at 60 m (Table 2). The highest POC loss rate (36%) and sinking velocity (12 m d^{-1}) were found during Autumn I (Table 2). The C/N ratio of sinking material suggested the sedimentation of degraded material during Winter II–III and Autumn I (C/N ratio: 10–15), while the sinking material had C/N ratios similar to those of the suspended biomass (C/N ratio: 6–8, Table 3) during Spring I–III, suggesting vertical flux of recently produced biomass.

3.4. Particle size and volume flux

Volume flux spectra (Fig. 5) provide information on the characteristics of sinking particles in the form of particle size (and volume) distribution and frequency. The area under the curve in the volume flux spectra corresponds to the total particle volume sinking out at a particular sampling date and depth. Our data show that the volume flux tended to be highest at 60 m and lowest at 30 m (except during Spring III). During Winter I, the largest particles were found in the 2.23 mm ESD_{image} size bin (Table A1), and a total volume flux of 312–545 × 10^3 mm^{-3} m^{-2} d^{-1} was estimated for the different sediment trap depths (Fig. 5). The ellipsoidal volume calculation method (Wiedmann et al., 2014) precluded estimation of the median size of the volume flux per depth, as an ellipsoidal volume could not be converted back to one definite particle ESD_{image}. Thus, we can only state that medium-sized and large particles (Fig. 5, Table A1) contributed most to the volume flux at 30 m and 40 m during Winter I, while

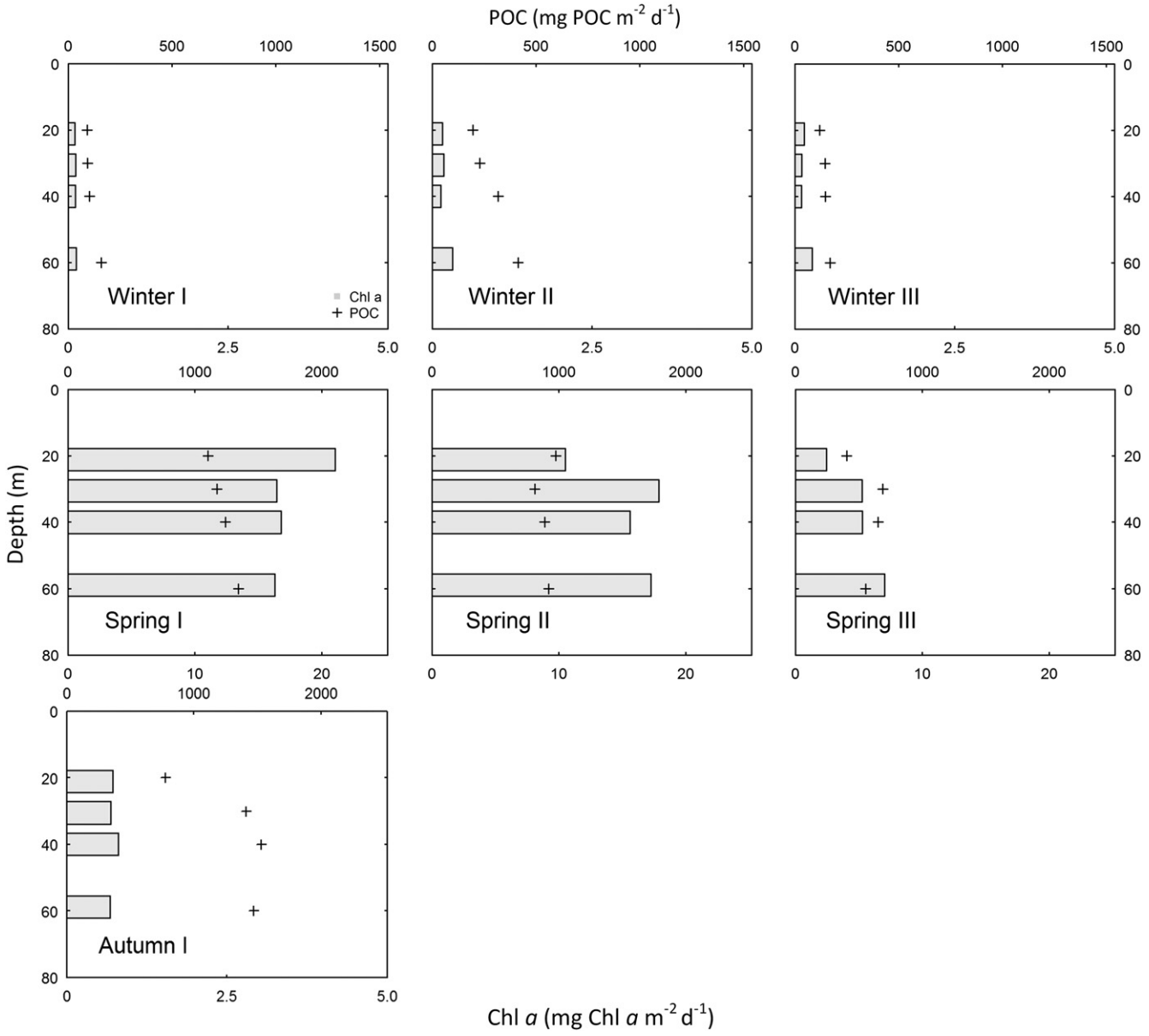

Fig. 4. Vertical flux of chlorophyll *a* (Chl *a*, gray bars) and particulate organic carbon (POC, black crosses) at 20, 30, 40, and 60 m during Winter I–III , Spring I–III, and Autumn I. Note different scale on the upper *x*-axis during Winter I–III and the lower *x*-axis for Spring I–III.

large particles were important at 20 m and 60 m. During Spring II, medium-sized particles were important contributors to the vertical volume flux down to 40 m, but extra-large particles were also found at 60 m (4.56 mm ESD_{image} size bin). Accordingly, the volume flux spanned from 171 to 1,195 $\times 10^3$ mm^{-3} m^{-2} d^{-1}. During Spring III, all of the particles were small to medium-sized and found in size bins ≤ 1.81 mm ESD_{image} (apart from one single particle at 20 m with 5.15 mm ESD_{image}), and the total volume flux was moderate, being 640–736 $\times 10^3$ mm^{-3} m^{-2} d^{-1} (Fig. 5). Autumn I was characterized by medium-sized sinking particles (bins ≤ 1.44 mm ESD_{image}) at 20 m and 30 m. Extra-large particles (≤3.62 mm ESD_{image} size bin) were found at 40 and 60 m, where also the highest volume fluxes of the present study were estimated (2,148 and 6,189 $\times 10^3$ mm^{-3} m^{-2} d^{-1}, respectively, Fig. 5). The semi-quantitative visual inspection of the gels

Table 2
Loss rate and average sinking velocity of chlorophyll *a* (Chl *a*) and particulate organic carbon (POC).

	Winter I		Winter II		Winter III		Spring I		Spring II		Spring III		Autumn I	
	30 m	60 m	30 m	60 m	30 m	60 m	30 m	60 m	30 m	60 m	30 m	60 m	30 m	60 m
Loss rate (% d^{-1})														
Chl *a*	9.5	5.1	9.6	8.1	6.0	8.3	–	–	15.5	7.8	19.7	9.6	6.6	3.7
POC	6.3	5.6	6.8	5.5	6.9	4.1	13.2	8.3	7.6	5.0	5.1	2.4	36.8	21.2
Average sinking velocity (m s^{-1})														
Chl *a*	2.8	3.1	2.8	4.6	1.7	6.6	–	–	4.2	5.6	3.8	4.2	2.4	2.8
POC	2.0	3.7	1.6	3.0	2.0	2.6	4.6	5.6	2.7	3.9	1.6	2.2	12.0	15.7

Table 3
Quality of the sinking material denoted by the C/N ratio (particulate organic nitrogen values for Winter I not available) and the most frequent particle type (detritus = mainly small, unidentifiable particles, PP = phytoplankton, FP = fecal pellets) in the deployed gel jars. Dominant particle type in bold. Number after the pteropod *Limacina* sp. specify the number of observed individuals in the gels.

		Winter I	Winter II	Winter III	Spring I	Spring II	Spring III	Autumn I
C/N	20, 30, 40, 60 m		10.6–12.4	12.7–14.1	7.9–8.0	6.8–7.8	6.7–7.2	13.0–15.0
Particle type	20 m	Detritus				Detritus, FP	PP aggregates, detritus	FP, aggregates,[a] *Limacina* sp. (138)
	30 m	Detritus, *Limacina* sp. (10)				Detritus, aggregates[a]	PP aggregates, detritus	Aggregates,[a] FP, *Limacina* sp. (63)
	40 m	Detritus				Detritus, aggregates[a]	Aggregates,[a] FP	Detritus, aggregates,[a] FP, *Limacina* sp. (73)
	60 m	Detritus, *Limacina* sp. (13)				Detritus, aggregates	FP, aggregates[a]	Detritus, aggregates, few FP, *Limacina* sp. (68)

[a] Most likely phytoplankton aggregates.

indicated that fine, degraded detritus dominated the vertical flux during Winter I (Fig. 6). The material was accompanied by some individuals of the pteropod *Limacina* sp. (characterized as swimmers and not included in the vertical flux estimates). Detrital material was still observed in the gel deployed during Spring II, but phytoplankton aggregates were also found. Phytoplankton aggregates dominated the observed particles in the gels deployed during Spring III, but they occurred together with detritus and fecal pellets. During Autumn I, a mixture of aggregates (probably phytoplankton), fecal pellets and detritus prevailed in the gels, as well as a substantial number of *Limacina* sp. individuals (138 at 20 m).

4. Discussion

The investigation of the seasonality in vertical biomass flux and particle characteristics showed that some of the seasonal drivers, such as phytoplankton blooms, were similar in ice-free fjords, be they arctic, subarctic, and boreal. However, glacial runoff affected sinking particles characteristics and apparently provided one important driver for the vertical carbon flux in the ice-free arctic Adventfjorden during the melt period.

4.1. Seasonal variation of suspended biomass in Adventfjorden—reflecting typical high latitude seasonality?

The arctic fjord, Adventfjorden, influenced by the Atlantic-derived West Spitsbergen Current, showed a pronounced seasonal variation during the 9 months covered by the present study. We used the high-frequency sampling program of hydrography and suspended biomass (blue triangles, Fig. 2, Table 1) as an environmental and ecological framework to categorize the seven field periods of this study into distinct seasons: winter, spring, and autumn.

The polar night at high latitudes prevents primary production and autotrophic biomass built-up through light limitation, which is caused by negligible sun light and deep mixing processes (e.g., induced by wind or thermal convection. The low Chl *a* and POC concentrations found during Winter I–III (Figs. 2 and 3) were thus typical for a high latitude winter situation and corresponded to previous observations around Svalbard (Iversen and Seuthe, 2011; Zajączkowski et al., 2010), in the Barents Sea (Olli et al., 2002) and in fjords in northern Norway (Eilertsen and Degerlund, 2010; Noji et al., 1993; Table 4). The phytoplankton spring bloom at IsA began in April in waters that were nutrient replenished (4.5 μM nitrate, Kubiszyn et al., in preparation), cold, non-stratified (Fig. 2), with a deep euphotic zone (Table 1), a setting comparable to reports from other high latitude regions (Eilertsen, 1993; Townsend et al., 1992). Parsons and Lalli (1988) related high surface concentrations of phytoplankton during an early bloom phase to low zooplankton abundance and a weak top-down regulation. Because we experienced this situation during Spring I in late April (high Chl *a* surface concentration, Fig. 3, and low zooplankton abundance, approximately 4×10^3 individuals m^{-3}, E.I. Stübner, pers. comm.), we characterized Spring I as a typical representation of an early bloom. Based on the low, but not yet depleted nitrate and silicate concentrations (1.5 μM nitrate + nitrite, 0.3 μM silicate, Kubiszyn et al., in preparation) in combination with the high Chl *a* concentrations at 25 m (Figs. 2 and 3), we classified Spring II in mid-May as a peak bloom situation. This categorization was further bolstered by the phytoplankton mixture (diatoms *Chaetoceros socialis* and *Thalassiosira nordenskioeldii* accompanied by the prymnesiophyte *P. pouchetii*, Kubiszyn et al., in preparation) because these species have been described as typical spring bloom species in north Norwegian fjords, the waters around Svalbard and in the Barents Sea (Degerlund and Eilertsen, 2010). During Spring III in late May, nitrate, the nutrient mainly limiting primary production in the Arctic (Tremblay and Gagnon, 2009), was depleted at 25 m, and silicate concentrations were low (0.9 μM, Kubiszyn et al., in preparation). These nutrient concentrations may have limited primary production, but this parameter was not measured during this study. Further, the abundant and diverse zooplankton community (approximately 20×10^3 individuals m^{-3}), of which 40–70% were meroplanktonic nauplii and larvae (Stübner et al., in revision; E.I. Stübner pers. comm.) most likely exerted a strong top-down regulation on phytoplankton and reduced the suspended Chl *a* concentration (Fig. 3). Accordingly, we classified Spring III as a late bloom stage. Stratification broke down due to cooling before Autumn I in mid-September. This caused a replenishment of the nutrients in the upper water column (e.g., 25 m: 2.6 μM nitrate, 2.5 μM silicate, Kubiszyn et al., in preparation), but no autotrophic biomass build-up was observed (Fig. 3). We cannot determine whether this was a result of low production rates or high loss rates (e.g., grazing from moderately abundant zooplankton: approximately 7×10^3 individuals m^{-3}, Stübner et al., in revision), but Autumn I was nonetheless considered to be a typical autumn situation because it matched an autumn scenario reported from Kongsfjorden, another fjord on western Svalbard (Iversen and Seuthe, 2011).

Suspended biomass concentrations at IsA corresponded well with a wide range of localities, including the open and central Barents Sea (Olli et al., 2002), fjords in western Svalbard (Kongsfjorden, Iversen and Seuthe, 2011), in northern Norway (Balsfjorden/ Malangen, Eilertsen and Degerlund, 2010; Ramfjorden, Noji et al., 1993; Balsfjorden, Reigstad and Wassmann, 1996; Malangen, Wassmann et al., 1996), in western Norway (Fanafjorden, Wassmann, 1984) and in the Conception Bay, Canada (Thompson et al., 2008, Table 4). Some differences in the intensity of the spring bloom concentrations were noted (e.g., , present study: 0.6–4.2 mg Chl *a* m^{-3}; Iversen and Seuthe, 2011, Kongsfjorden: 0.2–10 mg Chl *a* m^{-3}), but these were probably related to the inter-annual variability of Chl *a* concentration at high latitudes (Hodal et al., 2012; Stramska, 2005) and our sampling resolution (time, depth), which may have missed the most extreme Chl *a* concentrations at IsA station. Suspended Chl *a* and POC concentrations from the shallow innermost part of Adventfjorden (40 m, approximately 400 m from the mouths of Advent River and Longyear River) measured during winter 2006/ 2007 and autumn 2007 (Zajączkowski et al., 2010) exceeded the

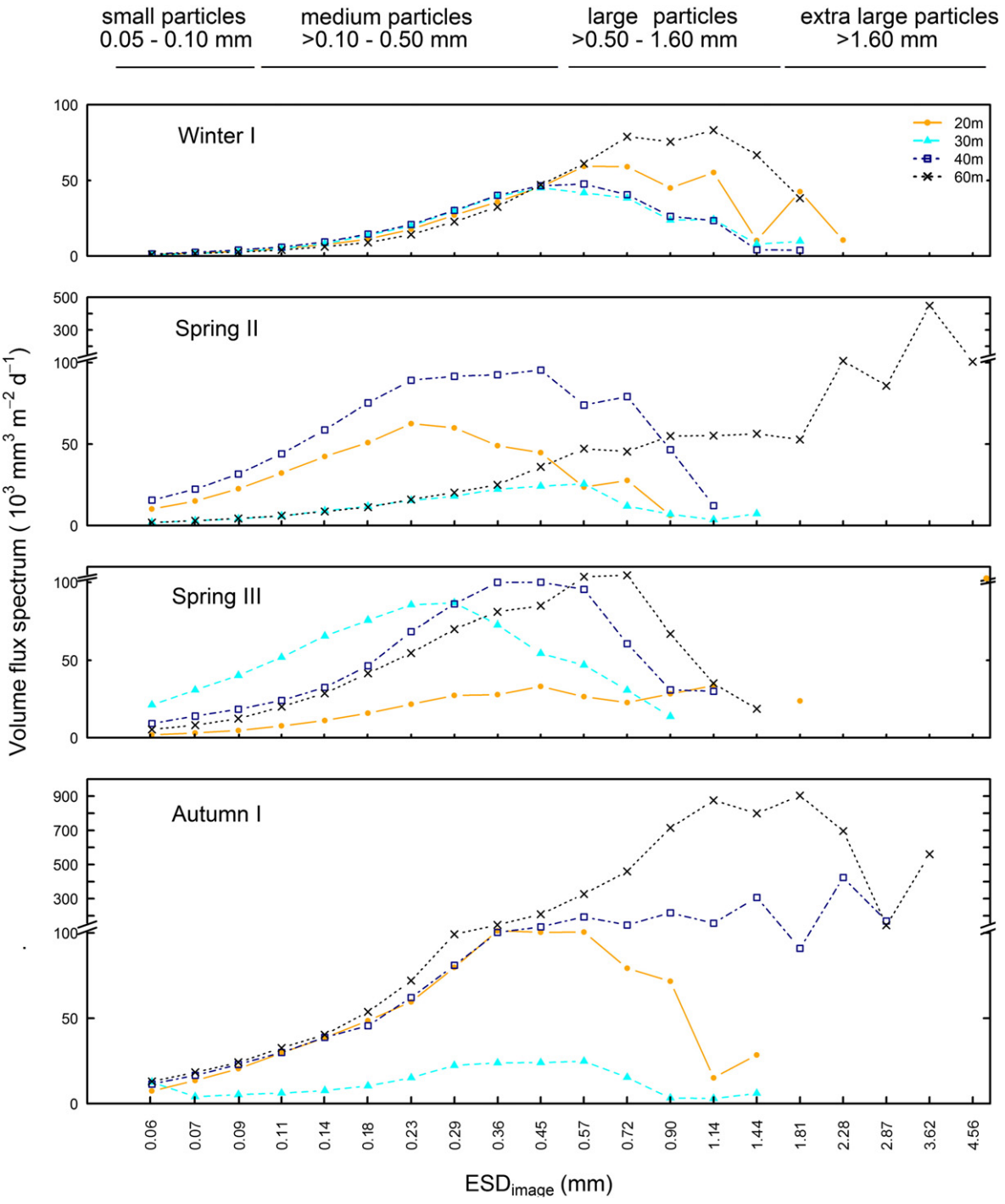

Fig. 5. Volume flux spectra at the four trap deployment depths (20 m: orange solid, 30 m: turquoise stippled, 40 m: blue dotted/stippled, 60 m: black dotted) during Winter I, Spring II, Spring III, and Autumn I. The horizontal axis is logarithmic and displays the average size of the particle bins. The area under the curve reflects the total volume of particles sinking out per sampling depth, and the top line indicates the size classes of the particles. Note the broken *y*-axis in Spring II, Spring III, and Autumn I.

concentrations found at IsA during the corresponding seasons in 2011/2012. The high C/N ratios in the shallow head of Adventfjorden suggest that local resuspension of previously sedimented allochthonous bottom material was probably enhanced in this area during winter and autumn (e.g., by thermal convection or tidal mixing, Zajączkowski et al., 2010; Zajączkowski and Włodarska-Kowalczuk, 2007) and contributed to the high suspended biomass.

In conclusion, comparison with the literature showed that the seasonal dynamics of suspended biomass in Adventfjorden was comparable to that in ice-free subarctic and arctic fjords and reflected a typical high latitude seasonality of low suspended biomass during winter and a maximum during the spring bloom.

4.2. Seasonality of the vertical flux intensity (POC, Chl a) in Adventfjorden—congruent with other ice-free high latitude regions?

Short-term sediment traps can be used to estimate vertical Chl *a* and POC flux, and if equipped with gel jars, they may give insight into the characteristics of the sinking particles. Combined with data on suspended biomass, data from the sediment traps can help to

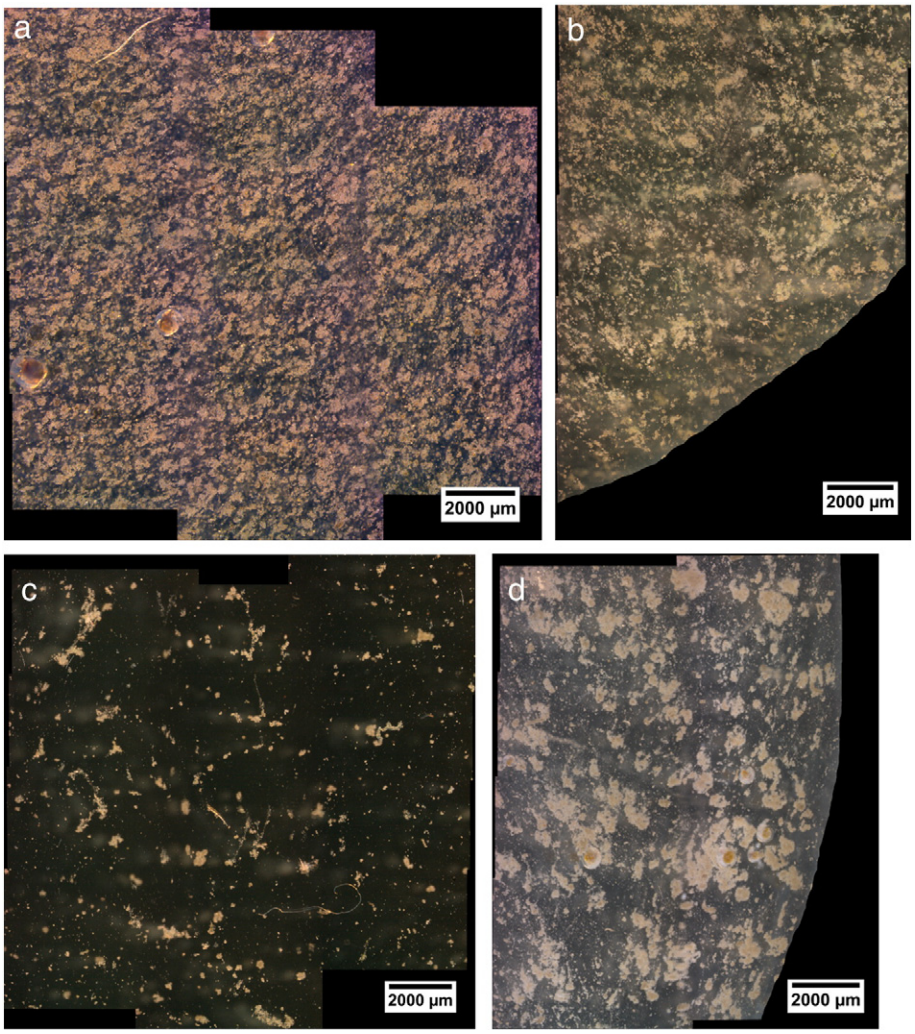

Fig. 6. Example images (15× magnification) demonstrating the different quality of sinking particles observed in the gel traps deployed at 60 m during Winter I (a), Spring II (b), Spring III (c), and Autumn I (d). Note that the December sample was deployed for approximately 24 h, while the other samples were only deployed for approximately 2 h.

understand the flux regulation, but traps deployed for a short time give only a snapshot picture; they cannot be assumed to provide robust seasonal flux patterns. We therefore compared the results from studies in other ice-free high latitude regions with the vertical flux seasonality observed at IsA to investigate if Adventfjorden resembled these areas.

Chl *a* and POC fluxes at IsA during winter were similar to those observed in the subarctic Ramfjorden (northern Norway, Noji et al., 1993), in the boreal Fanafjorden (western Norway, Wassmann, 1984) and in the central Barents Sea, an open arctic shelf sea (Olli et al., 2002; Table 4). The vertical POC flux in the shallow innermost part of Adventfjorden exceeded the POC flux at IsA considerably (Zajączkowski et al., 2010: approximately 500–750 mg POC m^{-2} d^{-1}; IsA: 90–400 mg POC m^{-2} d^{-1}; Table 4). We presume that this resulted from the resuspension of degraded marine and terrestrial material because of the high C/N ratios (up to 25) in the sinking material in the innermost Adventfjorden (Zajączkowski et al., 2010). Lower C/N rations in the sinking material at IsA (at the most 15) suggest a less pronounced resuspension effect in the mouth of the fjord (Table 3).

During spring, we observed strong pulses of vertical Chl *a* and POC flux, which exceeded previous measurements from the innermost Adventfjorden (Zajączkowski et al., 2010), the Balsfjorden and Malangen (northern Norway, Keck and Wassmann, 1996; Reigstad and Wassmann, 1996; Reigstad et al., 2000), the Fanafjorden (western Norway, Wassmann, 1984), and the Conception Bay (Canada, Thompson et al., 2008; Table 4). The fluxes were however comparable to those found in the Barents Sea (Olli et al., 2002; Table 4). We suggest that diatoms contributed to the strong vertical flux at IsA during early spring because they were abundant in the sediment traps during Spring I (molecular 454-sequencing analysis, M. Marquardt, pers. comm.) and they are known to produce sticky exopolymeric substances, which promote aggregate formation and sinking (Kiørboe et al., 1990; Smetacek, 1985; Thornton, 2002). Unfortunately, diatom sinking cannot be confirmed by direct observations of aggregates in the gel trap because the traps were deployed for a too long time during Spring I and the large amount of material on the gel made a particle size analysis impossible.

The vertical biomass flux decreased considerably from Spring I to Spring III, and we argue for a two-fold explanation of the decline in this flux during the course of the spring bloom (Fig. 4). First, the intensifying top-down regulation by zooplankton probably reduced the vertical flux from Spring I to III by reducing the biomass that could potentially settle (Fig. 4). Second, the shift in the phytoplankton bloom composition from diatom-dominated Spring I to *Phaeocystis*-dominated Spring III (Kubiszyn et al., in preparation) probably affected the vertical flux through the different sinking abilities of the two communities. The small-celled flagellate *P. pouchetii* dominated in the water column during Spring III (> 10^6 cells L^{-1}, Kubiszyn et al., in preparation) and cells of this species were also found in the sediment traps (454-sequencing, M. Marquardt, pers. comm.). However,

Table 4
Literature compilation of suspended POC and Chl *a* concentrations (mg m^{-3}) and the vertical flux of both parameters (mg m^{-2} d^{-1}) in high latitude fjords and the Barents Sea during winter, spring and autumn.

Place	Date	Depth (m)	Chl *a*	POC	C/N	Reference
Winter—suspended						
Adventfjorden—IsA, Svalbard	December '11/January '12	5,15,25,60	<0.1	50–160	8.3–11.7	Present study
Adventfjorden, Svalbard	November '06/February '07	5,35	0.2–0.6	180–500	2.5–20[a]	Zajączkowski et al. (2010)
Kongsfjorden, Svalbard	December '06	0–50[b]	0.01	43	6.6	Iversen and Seuthe (2011)
Central Barents Sea	March '98	0–50[b]	<0.05	40–70	7.4–9.0	Olli et al. (2002)
Balsfjorden, N-Norway	December '08	20,63	0.05			Eilertsen and Degerlund (2010)
Malangen, N-Norway	December '08	20,417	0.03–0.04			Eilertsen and Degerlund (2010)
Ramfjorden, N-Norway	November/December '89	0,10,30,50,70	0.03–0.20	70–270	13–25	Noji et al. (1993)
Spring—suspended						
Adventfjorden—IsA, Svalbard	April/May '12	5,15,25,60	0.6–4.2	230–630	6.2–7.1	Present study
Adventfjorden, Svalbard	April/May '06	5,35	0.1–6.8	300–900	6–16	Zajączkowski et al. (2010)
Kongsfjorden, Svalbard	April/May '06	0–50[b]	0.2–10	310–670	4.6–5.3	Iversen and Seuthe (2011)
Central Barents Sea	May '98	0–50[b]	4.5–7.5	300–680	6.5–8.0	Olli et al. (2002)
Balsfjorden, N-Norway	April '92	0–36[b]	2.7–4.1	500–830		Reigstad and Wassmann (1996)
Indrejord/ Tenneskjær, Malangen, N-Norway	April/May '91	0–30[b]	0.5–2.1			Wassmann et al. (1996)
Conception Bay, Newfoundland fjord, Canada	May '98	30	2.5			Thompson et al. (2008)
Autumn—suspended						
Adventfjorden—IsA, Svalbard	September '12	5,15,25,60	0.3–0.4	90–130	8.5–10.5	Present study
Adventfjorden, Svalbard	October '06	5,35	0.1	190–210	7.5–20[a]	Zajączkowski et al. (2010)
Kongsfjorden, Svalbard	September '06	0–50[b]	0.5	114	7.1	Iversen and Seuthe (2011)
Indrejord/ Tenneskjær, Malangen, N-Norway	September '91–October '91	0–30[b]	0.6–1.2			Wassmann et al. (1996)
Winter—sedimented						
Adventfjorden—IsA, Svalbard	December '11/January '12	20,30,40,60	<0.26	90–400	10.6–14	Present study
Adventfjorden, Svalbard	November '06/February '07	35	0.22–0.33	500–750	6–25	Zajączkowski et al. (2010)
Central Barents Sea	March '98	30–200[c]	<0.2	20–70		Olli et al. (2002)
Ramfjorden, N-Norway	November/December '89	10,30,50,70	0.03–0.3	25–300	9–12	Noji et al. (1993)
Fanafjorden, W-Norway	November '79/February '80	60,90		100–220	9–10	Wassmann (1984)
Spring—sedimented						
Adventfjorden—IsA, Svalbard	April/May '12	20,30,40,60[d]	2.5–20[d]	900–1350[d]	6.1–8.0	Present study
Adventfjorden, Svalbard	April/May '06	35	0.75–5	400–600	5–14	Zajączkowski et al. (2010)
Central Barents Sea	May '98	30–200[c]	10–30	200–2000		Olli et al. (2002)
Balsfjorden, N-Norway	April '92	30,60	0.5–5	180–630	6.5–13	Reigstad and Wassmann (1996)
Indrejord/ Tenneskjær, Malangen, N-Norway	April/May '91	30	0.1–13	250–750	5.5–10	Keck and Wassmann (1996)
Ullsfjorden, N-Norway	April '97	60	10–12	220–420	7.8–9.2	Reigstad et al. (2000)
Fanafjorden, W-Norway	April/May '91	60,90		220–600	8–13	Wassmann (1984)
Conception Bay, Newfoundland fjord, Canada	May '98	40,80		300–700	8–9	Thompson et al. (2008)
Autumn—sedimented						
Adventfjorden—IsA, Svalbard	September '12	20,30,40,60[d]	0.6–0.8[d]	770–1530[d]	13–15[d]	Present study
Adventfjorden, Svalbard	October '06	35	<0.1	500	7–16	Zajączkowski et al. (2010)
Indrejord/ Tenneskjær, Malangen, N-Norway	September '91–October '91	30		130–190	7.5–8.0	Keck and Wassmann (1996)
Fanafjorden, W-Norway	September '80	60,90		300–420	9.5	Wassmann (1984)

[a] Different size fractions (0.4–2.7 μm, 2.7–20 μm, and >20 μm).
[b] Average concentration, not integrated.
[c] 30, 40, 50, 60, 90, 120, 150, and 200 m.
[d] 2 h deployed traps not taken into account.

P. pouchetii cells have a low sinking velocity (approximately 1 m d^{-1}, Reigstad and Wassmann, 2007), and they mainly contribute to the vertical carbon flux above 90 m, when transported downwards by vertical mixing (Olli et al., 2002). The weak but present stratification during Spring III (Fig. 2) suggests that no strong deep mixing took place during this period, and we presume that a shift from fast-sinking diatoms (Passow, 1991) to slow-sinking detritus, including *Phaeocystis* cells, caused a reduction of the vertical POC flux during spring. This line of argumentation seems to be further supported by the decline in the biomass sinking velocities throughout spring (Table 2).

The interpretation of Autumn I data was complex. Glacial runoff occurs in Adventfjorden between June and September when air temperatures above 0 °C allow snow and glacial melting on land (Węsławski et al., 1999), and a tide- and wind-steered meandering glacial plume can be found in Adventfjorden (see reduced surface salinity in Figs. 2 and A1). The POC flux during Autumn I exceeded reported literature values by up to 30-fold (Table 4), and it was also higher than the flux observed during Springs I–III (Fig. 4). We suggest that the enhanced POC flux was linked to the glacial runoff. Zajączkowski et al. (2010) described an intense vertical flux of particulate inorganic and organic material in the shallow inner part of Adventfjorden during the summer melt period. Accordingly, we assume that entrained particulate organic matter also enhanced the POC flux at IsA. This is bolstered by a high C/N ratio in the sinking material in the present study during Autumn I (at most 15), which suggests sinking of degraded material (probably resuspended by e.g., estuarine circulation) or sinking of entrained terrestrial material (Table 3). Glacial melt water can also form "fingers" with a high concentration of total suspended particulate matter, stretching several kilometers from the mouth of Advent River into the fjord (Zajączkowski and Włodarska-Kowalczuk, 2007). This particulate matter may promote physical flocculation, a process in which unstable mineral particles, suspended in the entrained melt water, form aggregates with high sinking velocity (Kranck, 1973; Sutherland et al., 2015; Syvitski, 1980). Further, the lithogenic material was probably also incorporated into aggregates and fecal pellets in Adventfjorden, ballasted organic biomass through its high specific sinking velocity, as described from other regions (Iversen et al., 2010; Ploug et al., 2008), and increased the vertical POC flux at IsA.

The vertical Chl *a* and POC flux at IsA was congruent with the previously reported fluxes in other ice-free high latitude systems during winter and spring. However, the POC flux during autumn was much higher at IsA than described in the literature, and we suggest that this flux was driven by glacial runoff in Adventfjorden.

4.3. Sinking particle characteristics during different seasons

Drivers of physical and biological particle aggregation (e.g., shear, cell abundance, stickiness, Kiørboe et al., 1994) and modification by grazers (Turner, 2002, 2015) affect sinking particle characteristics (De La Rocha and Passow, 2007). Here, we discuss the characteristics of the sinking material such as the C/N ratio, the sinking velocity, and the POC: volume ratio at IsA during the different seasons and their possible drivers.

The C/N ratio, an indicator of the degradation stage of sinking material, matched well with the visual analysis of the gel jars deployed at IsA (Table 3). Degraded material (detritus) with a high C/N ratio was sinking out in mid-December (Winter I), while recently produced material (e.g., phytoplankton aggregates) with a C/N ratio closer to the Redfield ratio was observed in mid- and late May (Spring II and III, respectively, Table 3). During Autumn I, a high C/N ratio pointed toward sinking of strongly degraded material or terrestrial material, but visual inspection of the gel jars (20 m and 30 m) suggested sinking of aggregates and fecal pellets (Table 3). We presume that these different results were caused by the highly variable impact of the meandering glacial plume in Adventfjorden, and the fact that the two parameters (biochemical analyses and particle observations from gel traps) were measured in samples taken successively, not simultaneously. The high C/N ratios in the traps deployed for 24 h (13.0–15.0, Table 3) most likely resulted from a situation where the glacial plume covered IsA and a large amount of biomass with terrestrial origin was sinking out. In contrast, the aggregates and fecal pellets observed in the gel jars (which were deployed for 2 h), and the lower C/N ratios in the 2 h deployed sediment traps (6.5–8.8, data not shown) appear to emanate from a situation where the glacial plume did not hit IsA. The high variability of salinity and density on the two successive sampling days during Autumn I appears to bolster this assumption of a changing impact of the melt water plume (Fig. A1).

The sinking velocity is an important characteristic of the sedimenting material, as it determines the time a given particle is exposed to the pelagic community and potential grazing or degradation. The lower the sinking rate, the longer the exposure time for degradation. The average sinking velocity for total POC or Chl *a* biomass (Table 2) at IsA during winter and spring was comparable with the average velocities reported by Kiørboe et al. (1994) in the Danish Isefjorden (10 m), but somewhat higher than rates at Nordvestbanken (off the Norwegian Shelf, 100 m, Andreassen et al., 1999). Direct comparison of the average sinking velocity with particle sinking velocities, such as those estimated by Laurenceau-Cornec et al. (2015) or McDonnell and Buesseler (2010), is difficult because the calculations are based on different data (our study: integrated biomass and biomass flux; other studies: particle abundance in water column and sediment traps) and also differ in the size fraction included (our study: > 0.7 μm, Laurenceau-Cornec et al, 2015: > 150 μm, McDonnell and Buesseler, 2010: > 50 μm). According to Stokes' law, which tightly couples particle size and sinking velocity, the highest sinking rates in our study were expected at 60 m, where particles tended to be larger than at shallower depths (Fig. 5). Our calculations of the sinking velocity support this because a higher average sinking velocity was found at 60 m compared to 30 m (Table 2), but the coupling between particle size and sinking rates was not that straight forward. Extra-large particles were found both during Winter I and Autumn I (40, 60 m). During Autumn I (40, 60 m), the large particle size coincided with a high average sinking velocity (Table 2), but during Winter I the sinking velocity of the biomass was low even though large to extra-large particles were abundant. In contrast, although no extra-large particles were found in the 20 m and 30 m gels during Autumn I (Fig. 5), the average POC sinking velocity was high at 30 m (not calculated for 20 m). This underlined that sinking velocity is not influenced solely by particle size, but also a variety of other parameters such as sinking particle type, density, and mineral ballasting (De La Rocha and Passow, 2007; Iversen et al., 2010; Laurenceau-Cornec et al., 2015; McDonnell and Buesseler, 2010).

We suggest that incorporation of lithogenic material into organic particles (Iversen et al., 2010) and a higher abundance of fast-sinking fecal pellets (Table 3) outweighed the effect of size at the shallow sampling depths during Autumn I and resulted in the high sinking velocity. During Winter I, the low sinking velocity was apparently caused by the prevailing large, fluffy, detrital particles (Table 3) with low specific weight, combined with the lack of ballasting diatoms (Iversen and Ploug, 2010) or lithogenic material (no runoff during winter). An important implication of such a variable relationship between size and sinking rate becomes obvious when relating particle size or volume to the POC flux. For Winter I we calculated a low POC: volume ratio of approximately 0.0003 mg POC mm^{-3}, for the sinking particles, which reflects the strong contribution of fluffy detritus. The ratios from Spring II, characterized by smaller particles but high POC flux, were among the higher ratios observed during the present study (e.g., 30 m: 0.0050 mg POC mm^{-3}) and reflected the higher contribution of aggregates and fecal pellets. However, all POC: volume ratios at IsA were several magnitudes lower than ratios from the central Barents Sea, where sinking material comprised densely packed unidentifiable detritus and fecal material (0.0067–0.1101 mg POC mm^{-3}, Wiedmann et al., 2014). Accordingly, our study indicates that it is important to consider the type of particle when translating particle size or volume into POC flux.

Pteropods are another potentially important driver of sedimentation events at high latitudes. They have been observed during autumn and winter in the Fram Strait (24 individuals m^{-2} d^{-1} at 1700–2800 m, Meinecke and Wefer, 1990) and the Norwegian Sea (approximately 18×10^3 individuals m^{-2} d^{-1} at 50 m, Bathmann et al., 1991), matching pteropod abundances (approximately 8×10^3 m^{-2} d^{-1}, Table 3) encountered at IsA during Autumn I. Because our gel trap data did not indicate whether these pelagic gastropods were actively swimming or passively sinking into the trap cylinders, these animals were not regarded to represent a true component of the vertical biomass flux and removed from the image analyses. Nevertheless, pteropods may provide an important mechanism for vertical export, because their lost or rejected mucous feeding webs have been described to promote aggregate formation (Bathmann et al., 1991; Noji et al., 1997) and enhance the sinking velocity of organic matter.

In conclusion, our study shows that the average sinking velocity found at IsA corresponded to comparable studies in relevant fjord and arctic high latitude systems, but that coupling of particle size to the POC flux can be very challenging due to highly variable POC: volume ratios, influenced by biological and environmental factors. The meandering glacial plume during Autumn I apparently had a major effect on the sinking velocity of biomass, while the effect of pteropods on the downward POC flux in ice-free fjords needs further investigation.

4.4. Ecosystem functioning during different seasons in an high arctic ice-free fjord with a major glacial runoff during autumn

In the context of climate warming, it is likely that seasonally ice-covered arctic fjords and embayments may become permanently ice-free in the future. To predict the vertical flux intensity in these areas, an improved understanding is needed. We used Adventfjorden as a model area, because it has been seasonally ice-covered for several months during 2000–2005 (www.met.no, detailed ice maps available for Adventfjorden since 2000), but tended to be ice-free during the last years (2006–2007, 2010, 2012–2014). This lack of sea ice was probably a result of strong northerly winds, which enhanced the

advection of comparatively warm water from the West Spitsbergen Current into the fjords of western Svalbard (Cottier et al., 2007) as well as higher temperature of the advected water itself (Onarheim et al., 2014).

On the basis of our compiled data, we propose a conceptual model of the pelagic-benthic coupling in a year-round ice-free arctic fjord with glacial runoff during autumn (Fig. 7). In terms of suspended POC and Chl *a* concentrations, as well as the vertical biomass flux, the winter situation in Adventfjorden was comparable to that in boreal, subarctic and ice-free arctic fjords. We presume that mixing by thermal convection and wind must have been enhanced compared to the previous ice-covered situation and that detrital material, previously settled to the bottom, was re-suspended in the shallow areas and laterally advected to the middle of the fjord, as described for the subarctic Ramfjorden (Noji et al., 1993). Therefore, the vertical flux during the polar night was dominated by large detrital particles with a low density and low POC content, and in the absence of ballasting materials (e.g., diatom cells or lithogenic material), the sinking velocity and POC flux tended to be lower than during other seasons (Table 2, Figs. 4 and 7). The spring situation at IsA resembled previous observations from boreal, subarctic and arctic ice-free fjords in terms of suspended and sedimenting Chl *a* and POC. Strong vertical fluxes of un-grazed phytoplankton aggregates and detrital material were observed during the early bloom phase, but the vertical flux intensity decreased toward the late bloom. We suggest this was caused by the bloom shifting from being dominated by diatoms to being dominated by *P. pouchetii*, in combination with an intensifying top-down control by grazing zooplankton. During autumn, the ice-free Adventfjorden differed from many investigated fjords e.g., in northern Norway (Table 4), which are rarely affected by major glacial runoff (Fig. 2). We did not observe any autumn phytoplankton bloom, but we cannot be certain whether state if this was due to, e.g., lack of sufficient irradiance, or if our single autumn sampling simply missed the bloom. However, the sediment laded melt water input was identified as a major driver of the high POC flux during autumn. Further, high abundances of *Limacina* sp. and their rejected or lost mucous nets are potential additional drivers of the high POC flux.

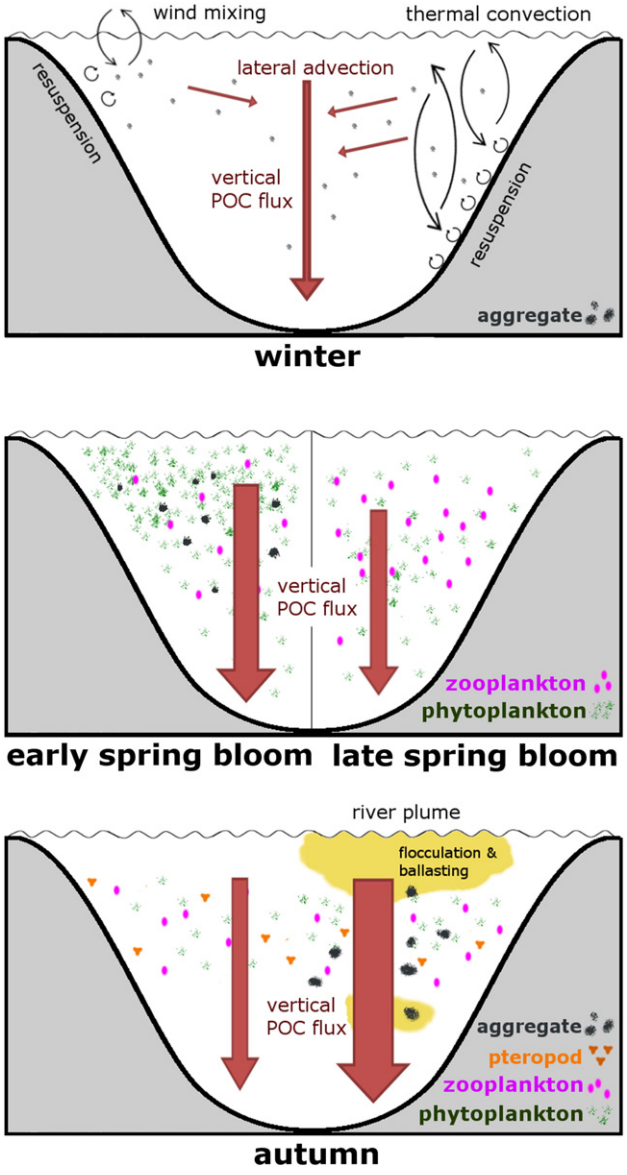

Fig. 7. Conceptual model of vertical POC flux during the different seasons in the ice-free, high Arctic Adventfjorden. Resuspension of detritus from the bottom and lateral advection resulted in some vertical POC flux during winter. A strong flux event can take place during an early spring bloom situation, when aggregates of phytoplankton and detritus are formed and sink out. During a late bloom phase, a stronger coupling between phytoplankton production and zooplankton diminishes the vertical POC flux. During autumn, the plume of glacial runoff can cause flocculation and aggregate formation. Entrained lithogenic material incorporated into sinking particles can enhance the sinking velocity of organic material as well as high pteropod abundances.

In summary, we propose that the seasonal vertical flux patterns in an ice-free arctic fjord with a glacial runoff resemble those in subarctic fjords during winter and spring. During autumn, however, the systems differ and a major POC sedimentation may be caused by the glacial runoff. In a scenario of climate warming previously ice-covered fjords and embayments may turn into permanently open waters. Ice algae blooms associated with the sea ice will then no longer occur and their contribution to the vertical carbon flux will cease. However, fjords affected by glacial runoff may still have strong POC sedimentation because the entrained sediment-loaded glacial runoff can drive vertical biomass flux during the melt season.

Supplementary data to this article can be found online at http://dx.doi.org/10.1016/j.jmarsys.2015.10.003.

Acknowledgments

We would like to thank the captain and the crew of the Norwegian coast guard vessel *K/V Svalbard*, *R/V Helmer Hanssen*, *M/S Viking*, and *M/S Farm* for great assistance during sampling under the sometimes harsh conditions. A helping hand was highly appreciated in the field (E. I. Stübner), during the CHN analyses (S. Øygarden), and with the hydrographical data (R. Skogseth). We also thank A. M. Kubiszyn and E. I. Stübner for insight in their plankton data and two anonymous reviewers for their comments, which improved this work substantially. The fieldwork was partly funded by the Arctic Field grant (RIS 5264) and the CONFLUX project (Tromsø Forskningsstiftelse).

References

Alldredge, A.L., Silver, M.W., 1988. Characteristics, dynamics and significance of marine snow. Prog. Oceanogr. 20, 41–82. http://dx.doi.org/10.1016/0079-6611(88)90053-5.

Andreassen, I.J., Wassman, P., Ratkova, T.N., 1999. Seasonal variation of vertical flux of phytyoplankton and biogenic matter at Nordvestbanken, north Norwegian shelf in 1994. Sarsia 84, 227–238.

Arrigo, K.R., 2014. Sea ice ecosystems. Ann. Rev. Mar. Sci. 6, 439–467. http://dx.doi.org/10.1146/annurev-marine-010213-135103.

Bathmann, U.V., Noji, T.T., von Bodungen, B., 1991. Sedimentation of pteropods in the Norwegian Sea in autumn. Deep-Sea Res. I 38, 1341–1360. http://dx.doi.org/10.1016/0198-0149(91)90031-A.

Bianchi, T.S., 2006. Biochemistry of Estuaries. Oxford University Press, Cary, USA (720 pp.).

Cottier, F.R., Nilsen, F., Inall, M.E., Gerland, S., Tverberg, V., Svendsen, H., 2007. Wintertime warming of an Arctic shelf in response to large-scale atmospheric circulation. Geophys. Res. Lett. 34. http://dx.doi.org/10.1029/2007GL029948 (L10607).

De La Rocha, C.L., Passow, U., 2007. Factors influencing the sinking of POC and the efficiency of the biological carbon pump. Deep-Sea Res. II 54, 639–658. http://dx.doi.org/10.1016/j.dsr2.2007.01.004.

Degerlund, M., Eilertsen, H.C., 2010. Main species characteristics of phytoplankton spring blooms in NE Atlantic and Arctic Waters (68–80°N). Estuar. Coasts 33, 242–269. http://dx.doi.org/10.1007/s12237-009-9167-7.

Ebersbach, F., Trull, T.W., 2008. Sinking particle properties from polyacrylamide gels during the Kerguelen Ocean and Plateau compared Study (KEOPS): zooplankton control of carbon export in an area of persistent natural iron inputs in the Southern Ocean. Limnol. Oceanogr. 53, 212–224. http://dx.doi.org/10.2307/40006162.

Eilertsen, H.C., 1993. Spring blooms and stratification. Nature 363, 24-24. http://dx.doi.org/10.1038/363024a0.

Eilertsen, H.C., Degerlund, M., 2010. Phytoplankton and light during the northern high-latitude winter. J. Plankton Res. 32, 899–912. http://dx.doi.org/10.1093/plankt/fbq017.

Eilertsen, H.C., Frantzen, S., 2007. Phytoplankton from two sub-Arctic fjords in northern Norway 2002–2004: I. Seasonal variations in chlorophyll *a* and bloom dynamics. Mar. Biol. Res. 3, 319–332. http://dx.doi.org/10.1080/17451000701632877.

Hodal, H., Falk-Petersen, S., Hop, H., Kristiansen, S., Reigstad, M., 2012. Spring bloom dynamics in Kongsfjorden, Svalbard: nutrients, phytoplankton, protozoans and primary production. Polar Biol. 35, 191–203. http://dx.doi.org/10.1007/s00300-011-1053-7.

Iversen, M.H., Ploug, H., 2010. Ballast minerals and the sinking carbon flux in the ocean: carbon-specific respiration rates and sinking velocity of marine snow aggregates. Biogeosciences 7, 2613–2624. http://dx.doi.org/10.5194/bg-7-2613-2010.

Iversen, K.R., Seuthe, L., 2011. Seasonal microbial processes in a high-latitude fjord (Kongsfjorden, Svalbard): I. Heterotrophic bacteria, picoplankton and nanoflagellates. Polar Biol. 34, 731–749. http://dx.doi.org/10.1007/s00300-010-0929-2.

Iversen, M.H., Nowald, N., Ploug, H., Jackson, G.A., Fischer, G., 2010. High resolution profiles of vertical particulate organic matter export off Cape Blanc, Mauritania: degradation processes and ballasting effects. Deep-Sea Res. I 57, 771–784. http://dx.doi.org/10.1016/j.dsr.2010.03.007.

Jackson, G.A., Maffione, R., Costello, D.K., Alldredge, A.L., Logan, B.E., Dam, H.G., 1997. Particle size spectra between 1 μm and 1 cm at Monterey Bay determined using multiple instruments. Deep-Sea Res. I 44, 1739–1767. http://dx.doi.org/10.1016/S0967-0637(97)00029-0.

Jackson, G.A., Waite, A.M., Boyd, P.W., 2005. Role of algal aggregation in vertical carbon export during SOIREE and in other low biomass environments. Geophys. Res. Lett. 32, L13607. http://dx.doi.org/10.1029/2005gl023180.

Ji, R., Jin, M., Varpe, Ø., 2013. Sea ice phenology and timing of primary production pulses in the Arctic Ocean. Glob. Chang. Biol. 19, 734–741. http://dx.doi.org/10.1111/gcb.12074.

Keck, A., Wassmann, P., 1996. Temporal and spatial patterns of sedimentation in the subarctic fjord Malangen, Northern Norway. Sarsia 80, 259–276.

Kiørboe, T., Andersen, K.P., Dam, H.G., 1990. Coagulation efficiency and aggregate formation in marine phytoplankton. Mar. Biol. 107, 235–245. http://dx.doi.org/10.1007/BF01319822.

Kiørboe, T., Lundsgaard, C., Olesen, M., Hansen, J.L.S., 1994. Aggregation and sedimentation processes during a spring phytoplankton bloom: a field experiment to test coagulation theory. J. Mar. Res. 52, 297–323. http://dx.doi.org/10.1357/0022240943077145.

Kranck, K., 1973. Flocculation of suspended sediment in the sea. Nature 246, 348–350. http://dx.doi.org/10.1038/246348a0.

Kubiszyn, A.M., Wiktor, J.M., Wiktor, J.M.J., Griffiths, C., Kristiansen, S., Gabrielsen, T.M., 2015n. The annual planktonic protist community structure in an ice-free high Arctic fjord (Adventfjorden, West Spitsbergen). J. Plankton Res. (in preparation).

Lampitt, R.S., 2001. Marine snow. In: Steele, J.H., Thorpe, S.A., Turekian, K.K. (Eds.), Encyclopedia of Ocean Sciences. Academic Press, San Diego, USA, pp. 1667–1675 http://dx.doi.org/10.1006/rwos.2001.0218.

Laurenceau-Cornec, E.C., Trull, T.W., Davies, D.M., De La Rocha, C.L., Blain, S., 2015. Phytoplankton morphology controls on marine snow sinking velocity. Mar. Ecol. Prog. Ser. 520, 35–56. http://dx.doi.org/10.3354/meps11116.

Leu, E., Søreide, J.E., Hessen, D.O., Falk-Petersen, S., Berge, J., 2011. Consequences of changing sea-ice cover for primary and secondary producers in the European Arctic shelf seas: timing, quantity, and quality. Prog. Oceanogr. 90, 18–32. http://dx.doi.org/10.1016/j.pocean.2011.02.004.

Lundsgaard, C.M.O., Reigstad, M., Olli, K., 1999. Sources of settling material: aggregation and zooplankton mediated fluxes in the Gulf of Riga. J. Mar. Syst. 23, 197–210. http://dx.doi.org/10.1016/S0924-7963(99)00058-5.

Mantoura, R.F.C., Wright, S.W., Barlow, R.G., Cummings, D.E., 1997. Filtration and storage of pigments from microalgae. Monographs on oceanographic methodology. In: Jeffrey, S.W., Mantoura, R.F.C., Wright, S.W. (Eds.), Phytoplankton Pigments in Oceanography: Guidelines to Modern Methods. UNESCO Publishing, Paris.

McDonnell, A.M.P., Buesseler, K.O., 2010. Variability in the average sinking velocity of marine particles. Limnol. Oceanogr. 55, 2085–2096. http://dx.doi.org/10.4319/lo.2010.55.5.2085.

Meinecke, G., Wefer, G., 1990. Seasonal pteropod sedimentation in the Norwegian Sea. Palaeogeogr. Palaeoclimatol. 79, 129–147. http://dx.doi.org/10.1016/0031-0182(90)90109-K.

Noji, T.T., Estep, K.W., Macintyre, F., Norrbin, F., 1991. Image analysis of faecal material grazed upon by three species of copepods: evidence for coprorhexy, coprophagy and coprochaly. J. Mar. Biol. Assoc. UK 71, 465–480. http://dx.doi.org/10.1017/S0025315400051717.

Noji, T.T., Noji, C.I.-M., Barthel, K.-G., 1993. Pelagic-benthic coupling during the onset of winter in a northern Norwegian fjord. Carbon flow and fate of suspended particulate matter. Mar. Ecol. Prog. Ser. 93, 89–99.

Noji, T.T., Bathmann, U.V., Noji, T.T., Bathmann, U.V., Bodungen, B.v., Voss, M., Antia, A., Krumbholz, M., Klein, B., Peeken, I., Noji, C.I.-M., Rey, F., 1997. Clearance of picoplankton-sized particles and formation of rapidly sinking aggregates by the pteropod, *Limacina retroversa*. J. Plankton Res. 19, 863–875. http://dx.doi.org/10.1093/plankt/19.7.863.

Olli, K., Rieser, C.W., Wassmann, P., Ratkova, T., Arashkevich, E., Pasternak, A., 2002. Seasonal variation in vertical flux of biogenic matter in the marginal ice zone and the central Barents Sea. J. Mar. Syst. 38, 189–204. http://dx.doi.org/10.1016/S0924-7963(02)00177-X.

Onarheim, I.H., Smedsrud, L.H., Ingvaldsen, R.B., Nilsen, F., 2014. Loss of sea ice during winter north of Svalbard. Tellus A 66, 23933. http://dx.doi.org/10.3402/tellusa.v66.23933.

Otsu, N., 1979. A threshold selection method from gray-level histograms. IEEE Trans. Syst. Man Cybern. 9, 62–66. http://dx.doi.org/10.1109/TSMC.1979.4310076.

Parsons, T.R., Lalli, C.M., 1988. Comparative oceanic ecology of the plankton communities of subarctic Atlantic and Pacific Oceans. Oceanogr. Mar. Biol. Annu. Rev. 26, 317–359.

Passow, U., 1991. Species-specific sedimentation and sinking velocities of diatoms. Mar. Biol. 108, 449–455. http://dx.doi.org/10.1007/BF01313655.

Passow, U., De La Rocha, C.L., 2006. Accumulation of mineral ballast on organic aggregates. Global Biogeochem. Cycles 20. http://dx.doi.org/10.1029/2005GB002579 (GB1013).

Passow, U., Wassmann, P., 1994. On the trophic fate of *Phaeocystis pouchetii* (Hariot): IV. The formation of marine snow by *P. pouchetii*. Mar. Ecol. Prog. Ser. 104, 153–161.

Ploug, H., Iversen, M.H., Fischer, G., 2008. Ballast, sinking velocity, and apparent diffusivity within marine snow and zooplankton fecal pellets: Implications for substrate turnover by attached bacteria. Limnol. Oceanogr. 53, 1878–1886. http://dx.doi.org/10.4319/lo.2008.53.5.1878.

Rat'kova, T.N., Wassmann, P., 2002. Seasonal variation and spatial distribution of phyto- and protozooplankton in the central Barents Sea. J. Mar. Syst. 38, 47–75. http://dx.doi.org/10.1016/s0924-7963(02)00169-0.

Reigstad, M., Wassmann, P., 1996. Importance of advection for pelagic-benthic coupling in north Norwegian fjords. Sarsia 80, 245–257. http://dx.doi.org/10.1080/00364827.1996.10413599.

Reigstad, M., Wassmann, P., 2007. Does *Phaeocystis* spp. contribute significantly to vertical export of organic carbon? Biogeochemistry 83, 217–234. http://dx.doi.org/10.1007/s10533-007-9093-3.

Reigstad, M., Wassmann, P., Ratkova, T., Arashkevich, E., Pasternak, A., Øygarden, S., 2000. Comparison of the springtime vertical export of biogenic matter in three northern Norwegian fjords. Mar. Ecol. Prog. Ser. 201, 73–80. http://dx.doi.org/10.3354/meps201073.

Reigstad, M., Riser, C.W., Wassmann, P., Ratkova, T., 2008. Vertical export of particulate organic carbon: Attenuation, composition and loss rates in the northern Barents Sea. Deep-Sea Res. II 55, 2308–2319. http://dx.doi.org/10.1016/j.dsr2.2008.05.007.

Rynearson, T.A., Richardson, K., Lampitt, R.S., Sieracki, M.E., Poulton, A.J., Lyngsgaard, M.M., Perry, M.J., 2013. Major contribution of diatom resting spores to vertical flux in the sub-polar North Atlantic. Deep-Sea Res. I 82, 60–71. http://dx.doi.org/10.1016/j.dsr.2013.07.013.

Smayda, T.J., 1971. Normal and accelerated sinking of phytoplankton in the sea. Mar. Geol. 11, 105–122. http://dx.doi.org/10.1016/0025-3227(71)90070-3.

Smetacek, V.S., 1985. Role of sinking in diatom life-history cycles—ecological, evolutionary and geological significance. Mar. Biol. 84, 239–251. http://dx.doi.org/10.1007/bf00392493.

Smith, R.W., Bianchi, T.S., Allison, M., Savage, C., Galy, V., 2015. High rates of organic carbon burial in fjord sediments globally. Nat. Geosci. 8, 450–453. http://dx.doi.org/10.1038/ngeo2421.

Søreide, J.E., Leu, E., Berge, J., Graeve, M., Falk-Petersen, S., 2010. Timing of blooms, algal food quality and *Calanus glacialis* reproduction and growth in a changing Arctic. Glob. Chang. Biol. 16, 3154–3163. http://dx.doi.org/10.1111/j.1365-2486.2010.02175.x.

Stramska, M., 2005. Interannual variability of seasonal phytoplankton blooms in the north polar Atlantic in response to atmospheric forcing. J. Geophys. Res. 110, C05016. http://dx.doi.org/10.1029/2004JC002457.

Stübner, E.I., Søreide, J.E., Reigstad, M., Marquardt, M., Blachowiak-Samolyk, K., 2015. Year-round meroplankton dynamics in high-Arctic Adventfjorden, Svalbard. J. Plankton Res. (in revision).

Sutherland, B.R., Barrett, K.J., Gingras, M.K., 2015. Clay settling in fresh and salt water. Environ. Fluid Mech. 15, 147–160. http://dx.doi.org/10.1007/s10652-014-9365-0.

Svensen, C., Wexels Riser, C., Reigstad, M., Seuthe, L., 2012. Degradation of copepod faecal pellets in the upper layer: role of microbial community and *Calanus finmarchicus*. Mar. Ecol. Prog. Ser. 462, 39–49. http://dx.doi.org/10.3354/meps09808.

Syvitski, J.M., 1980. Flocculation, Agglomeration, and Zooplankton Pelletization of Suspended Sediment in a Fjord Receiving Glacial Meltwater. In: Freeland, H., Farmer, D., Levings, C. (Eds.), Fjord Oceanography. Springer, US, pp. 615–623.

Thiele, S., Fuchs, B.M., Amann, R., Iversen, M.H., 2015. Colonization in the photic zone and subsequent changes during sinking determines bacterial community composition in marine snow. Appl. Environ. Microbiol. 81, 1463–1471. http://dx.doi.org/10.1128/aem.02570-14.

Thompson, R.J., Deibel, D., Redden, A.M., McKenzie, C.H., 2008. Vertical flux and fate of particulate matter in a Newfoundland fjord at sub-zero water temperatures during spring. Mar. Ecol. Prog. Ser. 357, 33–49. http://dx.doi.org/10.3354/meps07277.

Thornton, D., 2002. Diatom aggregation in the sea: mechanisms and ecological implications. Eur. J. Phycol. 37, 149–161. http://dx.doi.org/10.1017/S0967026202003657.

Townsend, D.W., Keller, M.D., Sieracki, M.E., Ackleson, S.G., 1992. Spring phytoplankton blooms in the absence of vertical water column stratification. Nature 360, 59–62. http://dx.doi.org/10.1038/360059a0.

Tremblay, J.-É., Gagnon, J., 2009. The effects of irradiance and nutrient supply on the productivity of Arctic waters: a perspective on climate change. In: Nihoul, J.C.J., Kostianoy, A.G. (Eds.), nfluence of Climate Change on the Changing Arctic and Sub-Arctic Conditions. Springer, Netherlands, pp. 73–93.

Tremblay, C., Runge, J., Legendre, L., 1989. Grazing and sedimentation of ice algae during and immediately after a bloom at the ice-water interface. Mar. Ecol. Prog. Ser. 56, 291–300.
Turner, J.T., 2002. Zooplankton fecal pellets, marine snow and sinking phytoplankton blooms. Aquat. Microb. Ecol. 27, 57–102. http://dx.doi.org/10.3354/ame027057.
Turner, J.T., 2015. Zooplankton fecal pellets, marine snow, phytodetritus and the ocean's biological pump. Prog. Oceanogr. 130, 205–248. http://dx.doi.org/10.1016/j.pocean.2014.08.005.
Wassmann, P., 1984. Sedimentation and benthic mineralization of organic detritus in a Norwegian fjord. Mar. Biol. 83, 83–94. http://dx.doi.org/10.1007/BF00393088.
Wassmann, P., Peinert, R., Smetacek, V., 1991. Patterns of production and sedimentation in the boreal and polar Northeast Atlantic. Proceedings of the Pro Mare Symposium on Polar Marine Ecology, Trondheim, 12–16 May 1990. Pol. Res. 10, 209–228. http://dx.doi.org/10.1111/j.1751-8369.1991.tb00647.x.
Wassmann, P., Svendsen, H., Keck, A., Reigstad, M., 1996. Selected aspects of the physical oceanography and particle fluxes in fjords of northern Norway. J. Mar. Syst. 8, 53–71.
Węsławski, J.M., Kwasniewski, S., Wiktor, J., 1991. Winter in a Svalbard fjord ecosystem. Arctic 44, 115–123. http://dx.doi.org/10.14430/arctic1527115-123.
Węsławski, J.M., Szymelfenig, M., Zajączkowski, M., Keck, A., 1999. Influence of salinity and suspended matter of benthos of an Arctic tidal flat. ICES J. Mar. Sci. 56, 194–202 (Suppl.).
Wexels Riser, C., Wassmann, P., Reigstad, M., Seuthe, L., 2008. Vertical flux regulation by zooplankton in the northern Barents Sea during Arctic spring. Deep-Sea Res. II 55, 2320–2329. http://dx.doi.org/10.1016/j.dsr2.2008.05.006.
Weydmann, A., Søreide, J.E., Kwaśniewski, S., Leu, E., Falk-Petersen, S., Berge, J., 2013. Ice-related seasonality in zooplankton community composition in a high Arctic fjord. J. Plankton Res. 35, 831–842. http://dx.doi.org/10.1093/plankt/fbt031.
Wiedmann, I., Reigstad, M., Sundfjord, A., Basedow, S., 2014. Potential drivers of sinking particle's size spectra and vertical flux of particulate organic carbon (POC): turbulence, phytoplankton, and zooplankton. J. Geophys. Res. Oceans 119, 6900–6917. http://dx.doi.org/10.1002/2013JC009754.
Zajączkowski, M., Włodarska-Kowalczuk, M., 2007. Dynamic sedimentary environments of an Arctic glacier-fed river estuary (Adventfjorden, Svalbard). I. Flux, deposition, and sediment dynamics. Estuar. Coast. Shelf Sci. 74, 285–296. http://dx.doi.org/10.1016/j.ecss.2007.04.015.
Zajączkowski, M., Nygård, H., Hegseth, E.N., Berge, J., 2010. Vertical flux of particulate matter in an Arctic fjord: the case of lack of the sea-ice cover in Adventfjorden 2006–2007. Polar Biol. 33, 223–239. http://dx.doi.org/10.1007/s00300-009-0699-x.